Breakdown of autoresonance due to separatrix crossing in dissipative systems: From Josephson junctions to the three-wave problem

Ricardo Chacón
Departamento de Física Aplicada, Escuela de Ingenierías Industriales, Universidad de Extremadura, Apartado Postal 382, E-06071 Badajoz, Spain

(Received 13 June 2008; revised manuscript received 22 September 2008; published 17 December 2008)

Optimal energy amplification via autoresonance in dissipative systems subjected to separatrix crossings is discussed through the universal model of a damped driven pendulum. Analytical expressions of the autoresonance responses and forces as well as the associated adiabatic invariants for the phase space regions separated by the underlying separatrix are derived from the energy-based theory of autoresonance. Additionally, applications to a single Josephson junction, topological solitons in Frenkel-Kontorova chains, as well as to the three-wave problem in dissipative media are discussed in detail from the autoresonance analysis.

DOI: 10.1103/PhysRevE.78.066608 PACS number(s): 05.45.Yv, 02.70.−c, 42.65.−k, 45.10.Db

I. INTRODUCTION

Autoresonance (AR) induced energy amplification in nonlinear, driven, and deterministic systems occurs when the system continuously adjusts its amplitude so that its instantaneous nonlinear period matches the driving period. AR phenomena have been well known for about half a century and they have been observed in particle accelerators [1], planetary dynamics [2], nonlinear oscillators [3], and atomic and molecular physics [4], among many other fields where a Hamiltonian description is suitable. Regarding dissipative systems, an energy-based AR (EBAR) theory which explains in a unified frame many phenomenological and approximate results arising from a previous adiabatic approach to AR phenomena has been proposed recently [5]. This theory applies to the general family of systems

$$\ddot{x} = g[x,f(t)] - d(x,\dot{x}) + p(x,\dot{x})F(t), \qquad (1)$$

where $g[x,f(t)]=-\partial V/\partial t$ [$V(x,t)$ being an arbitrary potential], $-d(x,\dot{x})$ is a general damping force, and $p(x,\dot{x})F(t)$ is a general temporal force. The corresponding equation for the energy is

$$\dot{E} = \dot{x}[-d(x,\dot{x}) + p(x,\dot{x})F(t)] + \partial V/\partial t \equiv P(x,\dot{x},t),$$

where $E(t)\equiv \dot{x}^2/2+V(x,t)$ and $P(x,\dot{x},t)$ are the energy and power, respectively. The AR solutions are defined by imposing that the energy variation

$$\Delta E = \int_{t_1}^{t_2} P(x,\dot{x},t)dt$$

is a maximum (with t_1, t_2 arbitrary but fixed instants), which implies a necessary condition to be fulfilled by the AR solutions and excitations: the Euler equation

$$\frac{\partial P}{\partial x} = \frac{d}{dt}\left(\frac{\partial P}{\partial \dot{x}}\right). \qquad (2)$$

From Eq. (2) a relationship between x, $\dot{x}$, f, and F can be deduced such that the solutions of the system given by Eqs. (1) and (2) together provide the AR excitations $f_{\mathrm{AR}}(t)$, $F_{\mathrm{AR}}(t)$, and the AR solutions $x_{\mathrm{AR}}(t)$ (see Ref. [5] for more details). In particular, the application of the EBAR theory to a Duffing equation

$$\ddot{x} + \omega_0^2(x + bx^3) = -\delta\dot{x} + F(t)$$

shows that its AR excitations and solutions only exist if the relationship $\omega_0^2=2\delta^2/9$ is satisfied. This condition on ω_0 and δ is precisely the same condition for the equation providing the AR solutions

$$\ddot{x}_{\mathrm{AR}} + \omega_0^2(x_{\mathrm{AR}} + bx_{\mathrm{AR}}^3) = \delta\dot{x}_{\mathrm{AR}}$$

(see Ref. [5]), to present both a nontrivial Lie symmetry and the Painlevé property [6] which indicates that such an equation is integrable. As is well known, integrability and separatrix crossing (SC) are incompatible notions. Since SC is essential to understand many ubiquitous nonlinear phenomena including chaos [7], a relevant question naturally arises: How does AR work when a dissipative system crosses the separatrix associated with its underlying integrable counterpart?

In this work, this fundamental problem is studied through the universal model of a damped driven pendulum

$$\ddot{x} + \omega_0^2 f(t)\sin x = -\delta\dot{x} + F(t), \qquad (3)$$

where the as yet undetermined parametric $f(t)$ [8] and external $F(t)$ excitations have to be obtained conjointly to yield a maximal increase of the pendulum's energy over time. The functions $f(t)$ and $F(t)$ are k-times piecewise continuously differentiable. A first observation is that a lack of continuity of the AR solutions $x_{\mathrm{AR}}(t)$ across the separatrix is expected to arise because the period is infinite on the separatrix and therefore the requirement of continuous matching between the instantaneous pendulum period and the driving period is no longer possible across it.

The paper is organized as follows. AR analysis is applied to Eq. (3) in Sec. II, including analytical expressions of the AR excitations and forces. Section III gives the adiabatic invariants associated with the AR excitations and forces deduced in Sec. II. The application of the findings of previous sections to three physically meaningful situations is discussed in detail in Sec. IV. Finally, some concluding remarks are presented in Sec. V.

II. AUTORESONANCE ANALYSIS

The Euler condition [see Eq. (2)], corresponding to Eq. (3), and Eq. (3) together yield the equation governing the AR excitations and solutions

$$\ddot{x}_{AR} + \omega_0^2 f_{AR}(t)\sin x_{AR} = \delta\dot{x}_{AR} + \int \sin x_{AR} df_{AR}, \quad (4)$$

$$F_{AR}(t) = 2\delta\dot{x}_{AR} + \int \sin x_{AR} df_{AR}. \quad (5)$$

To obtain AR solutions [and hence AR excitations, see Eq. (5)], consider the ansatz $x_{AR}(t)=2\mathrm{am}[\omega_0^2 f_{AR}(t)+\varphi;m(t)]$, where am $(\cdot;m)$ is the elliptic amplitude of parameter m, and where the functions $f_{AR}(t)$, $m(t)$ have to be determined for the ansatz to satisfy Eq. (4), while φ is an arbitrary constant. This implies

$$\dot{x}_{AR}(t) = 2\dot{f}_{AR} dn[\Psi(t);m] + \dot{m}m^{-1}(1-m)^{-1}\{(1-m)\Psi(t) - E(\Psi(t);m)\}\mathrm{dn}[\Psi(t);m] + \dot{m}(1-m)^{-1}\mathrm{cn}[\Psi(t);m]\mathrm{sn}[\Psi(t);m],$$

where $\Psi(t) \equiv \omega_0^2 f_{AR}(t)+\phi$, $E(\cdot;m)$ is the elliptic integral of the second kind, and sn $(\cdot;m)$, cn $(\cdot;m)$, dn $(\cdot;m)$ are Jacobian elliptic functions of parameter m [9]. Now, one assumes that the temporal variation of $m(t)$ is sufficiently slow to allow one to drop the terms proportional to $\dot{m}(t)$ in the above expression for $\dot{x}_{AR}(t)$ and consistently obtain $m(t)$. In such a case, Eq. (4) reduces to

$$\ddot{x}_{AR} + \omega_0^2 e^{\delta t/3} \sin x_{AR} = (2\delta/3)\dot{x}_{AR}, \quad (6)$$

which has the solution

$$x_{AR}(t) = 2\mathrm{am}(\omega_0^2 f_{AR}(t) + \varphi; m(t))$$

and, hence,

$$F_{AR}(t) = (10\omega_0^2\delta^2/9) f_{AR}(t)\mathrm{dn}(\omega_0^2 f_{AR}(t) + \varphi; m(t))$$

[see Eq. (5)], with

$$f_{AR}(t) = e^{\delta t/3},$$

$$m(t) = 9\omega_0^{-2}\delta^{-2}e^{-\delta t/3}$$

satisfying the constraint $m\omega_0^2 f_{AR}=9\delta^{-2}$. Clearly, Eq. (6) is accurate only for $t>\tau\sim 1/\delta$ since $\dot{m}(t>\tau)\simeq 0$, while for $t<\tau$ one has $f_{AR}(t)\simeq 1$. Thus, after using well-known properties of the functions am $(\cdot;m)$ and dn $(\cdot;m)$ [9], one obtains the AR solutions and excitations

$$x_{AR}(t>\tau) = 2\omega_0^2 e^{\delta t/3} + 2\varphi,$$

$$F_{AR}(t>\tau) = (10\omega_0^2\delta^2/9)e^{\delta t/3}, \quad (7)$$

which are expected to be valid after SC (see theorem 2 below). The relationship $f_{AR}(t<\tau)\simeq 1$ suggests taking $f(t)=1$ in Eq. (3) to study AR before SC (see theorem 2 below). With this assumption, Eq. (4) reduces to

$$\ddot{x}_{AR} + \omega_0^2 \sin x_{AR} = \delta\dot{x}_{AR}, \quad (8)$$

for $t<\tau$ instead of Eq. (6). Notice that both Eq. (6) and Eq. (8) exhibit two symmetries:

$$\hat{S}_1: x \to -x,$$

$$\hat{S}_2: t \to -t, \quad \delta \to -\delta$$

[10]. Symmetry $\hat{S}_2$ implies that solutions of a damped pendulum are those of Eq. (8) under time reversal. Although no exact analytical solutions of Eq. (8) are known, the following result provides useful approximate solutions.

Theorem 1. For initial conditions sufficiently close to (but different from) the stable equilibrium of the integrable pendulum (δ=0), Eq. (8) has the solutions

$$x_{AR}(t<\tau) = Ae^{\delta t/2}\sin(\sqrt{\omega_0^2 - \delta^2/4}t + \varphi_0) + O(A^3), \quad (9)$$

and hence the AR excitations are $F_{AR}(t<\tau)=2\delta\dot{x}_{AR}(t<\tau)$ [see Eq. (5)], where A, φ_0 are arbitrary constants and $\omega_0 > \delta/2$.

Proof. Using the ansatz $x_{AR}=Ae^{\lambda t}\sin(\omega t+\varphi_0)$ together with the relationship $\sin(z\sin\theta)=2\sum_{k=0}^{\infty}J_{2k+1}(z)\sin[(2k+1)\theta]$ and the property $J_k(z\to 0)\sim(z/2)^k/\Gamma(k+1)$, $k\neq -1, -2, -3, \ldots$, where J_k are Bessel functions and $\Gamma(z)$ is the gamma function, solution (9) is straightforwardly obtained.

The physical meaning of the time constant δ^{-1} is now apparent: It represents the time scale in which the pendulum escapes in AR from the initial well, i.e., until an SC occurs. The following result provides an estimate of the escape time τ.

Theorem 2. The escape time τ from the initial well while the pendulum remains in AR scales as $\tau\sim\delta^{-1}$.

Proof. Equation (8) can be recast in the form $\dot{E}_{AR}=\delta\dot{x}_{AR}^2$, where $E_{AR}=\dot{x}_{AR}^2/2-\omega_0^2\cos x_{AR}$ is the energy. After integrating this equation till the escape time τ and applying the first mean value theorem, one straightforwardly obtains $\tau=[\Delta E_{AR}/\dot{x}_{AR}^2(t^*)]\delta^{-1}$, $0\leqslant t^*\leqslant\tau$, where $\Delta E_{AR}/\dot{x}_{AR}^2(t^*)$ depends on the initial conditions and ω_0.

Numerical experiments confirmed accurately the scaling $\tau\sim\delta^{-1}$ (see Fig. 1) and the above approximate AR solutions (see Figs. 2 and 3). The fact that Eq. (6) solely reduces to Eq. (8) for $t<\tau$ if $\delta\to 3\delta/2$, i.e., after rescaling the escape time τ, indicates the breakdown of the AR solutions due to SC. In other words, there is no smooth way to go from libration to full rotation while the pendulum remains in AR.

III. ADIABATIC INVARIANTS

The EBAR theory predicted the existence of an adiabatic invariant associated with the AR solutions of the aforementioned Duffing equation [5]. In the present case, one could expect to find different adiabatic invariants respectively associated with the two AR solutions (7) and (9). To this end, note that Eq. (8) can be derived from the Lagrangian

$$L = e^{-\delta t}(\dot{x}^2/2 + \omega_0^2\cos x)$$

whose associated Hamiltonian is

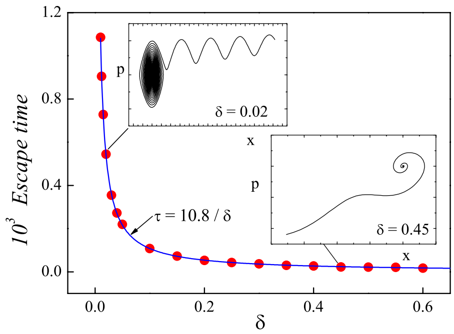

FIG. 1. (Color online) Numerically obtained escape time τ vs dissipation coefficient δ (dots) and analytical fit $\tau=10.8\delta^{-1}$ (see theorem 2, solid line) for a pendulum in AR [see Eq. (8)] with $\omega_0=1$ and fixed initial conditions. The two insets show the orbits in the phase space for δ=0.02 and δ=0.45, respectively. Note that the scaling δ^{-1} is valid over three orders of magnitude in τ.

$$H = p^2 e^{\delta t}/2 - \omega_0^2 e^{-\delta t}\cos x, \quad p \equiv \dot{x}.$$

The form of this Hamiltonian suggests the following simplifying canonical transformation:

$$X = xe^{-\delta t/2}, \quad P = pe^{\delta t/2},$$

which comes from the generating function

$$F_2(x,P,t) = xPe^{-\delta t/2}$$

[11]. The new Hamiltonian therefore reads

$$K(X,P,t) = P^2/2 - \omega_0^2 e^{-\delta t}\cos(Xe^{\delta t/2}) + \delta XP/2.$$

Thus, one obtains that the AR solutions are associated (in terms of the old canonical variables) with the adiabatic invariant

$$I = p^2/2 - \omega_0^2 \cos x + \delta xp/2 \tag{10}$$

long before SC, i.e., $dK/dt \simeq 0$ when $t \ll \tau$ (see Fig. 2). Note that this adiabatic invariant reduces to energy provided that dissipation is sufficiently small. Similarly, Eq. (6) can be derived from the Lagrangian

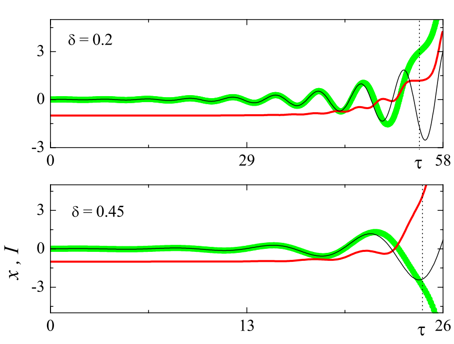

FIG. 2. (Color online) Exact AR solutions [see Eq. (8), thick line], approximate AR solutions [see Eq. (9), thin line], and adiabatic invariant I [see Eq. (10), medium line] vs time for δ=0.2 (top panel) and δ=0.45. Here, τ denotes the instant at which the pendulum escapes from the initial well, and $\omega_0=1$.

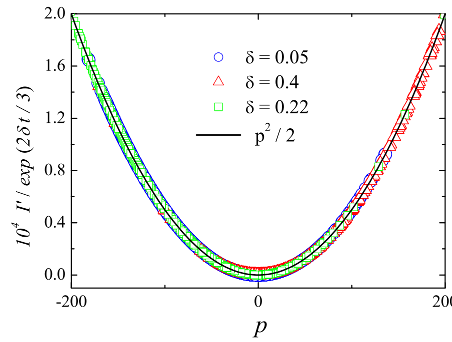

FIG. 3. (Color online) Adiabatic invariant associated with AR solutions outside the underlying separatrix I' [see Eqs. (6) and (11)] vs momentum p for three values of the dissipation coefficient: δ=0.05 (circles), δ=0.22 (squares), and δ=0.4 (triangles). The black line represents the prediction (12) obtained from the AR solutions (7). Here $\omega_0=1$.

$$L' = e^{-2\delta t/3}(\dot{x}^2/2 + \omega_0^2 e^{\delta t/3}\cos x)$$

with

$$H' = p^2 e^{2\delta t/3}/2 - \omega_0^2 e^{-\delta t/3}\cos x$$

being the associated Hamiltonian. Now, the generating function

$$F_2'(x,P,t) = xPe^{-\delta t/3}$$

yields the canonical transformation

$$X = xe^{-\delta t/3}, \quad P = pe^{\delta t/3}.$$

Therefore, the new Hamiltonian reads

$$K'(X,P,t) = P^2/2 - \omega_0^2 e^{-\delta t/3}\cos(Xe^{\delta t/3}) + \delta XP/3.$$

When $t \gg \tau$, one sees that K' is almost conserved ($dK'/dt \simeq 0$), i.e., the AR solutions are associated (in terms of the old canonical variables) with the adiabatic invariant

$$I' = p^2 e^{2\delta t/3}/2 + \delta xp/3 \tag{11}$$

long after SC. Since I' becomes larger and larger as K' is better and better conserved, one expects

$$I' e^{-2\delta t/3} \approx p^2/2 + 4\delta^2\omega_0^4/9 \tag{12}$$

according to the above prediction for $x_{AR}(t > \tau)$ [see Eq. (7)]. Figure 3 shows how numerical simulations accurately confirmed the prediction (12). After SC, the branch of the parabola with $p>0$ ($p<0$) is associated with clockwise (counterclockwise) AR rotations. Whether the AR rotations have one or the other sense depends upon the initial conditions, as can be appreciated in Fig. 4, where it is also apparent that the escape time strongly depends upon those conditions for fixed δ and ω_0.

IV. APPLICATIONS

The results of the previous sections can be directly applied to a mechanical pendulum. The present section discusses their detailed application to three additional, physi-

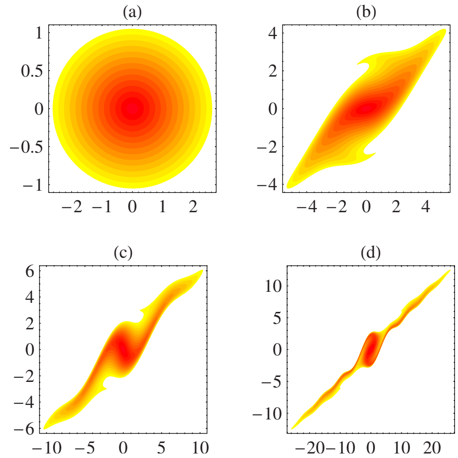

FIG. 4. (Color online) Phase space (x-p) AR trajectories [see Eq. (8)] starting from 3×10^3 initial conditions uniformly distributed on an ellipse centered at the origin at successive instants: $t=0$ (a), $t=1.2/\delta$ (b), $t=1.6/\delta$ (c), and $t=2.3/\delta$ (d). Here, $\delta=0.4$, $\omega_0=1$.

cally meaningful contexts: The three-wave problem in dissipative media, the resistively and capacitively shunted junction model, and the Frenkel-Kontorova model.

A. Three-wave problem in dissipative media

The three-wave interaction plays a fundamental role in physics because it represents lowest-order (in terms of wave amplitudes) nonlinear effects in systems approximately described by a linear superposition of discrete waves. In particular, the resonant nonlinear interaction of three collinear plane waves in a dissipative medium [12] is described by the real amplitude ($a_j, j=0,1,2$) equations (with $\partial_t \equiv \partial/\partial t$, etc.)

$$(\partial_t + v_0\partial_x + \Gamma_0)a_0 = -\beta_0 a_1 a_2,$$

$$(\partial_t + v_1\partial_x + \Gamma_1)a_1 = \beta_1 a_0 a_2,$$

$$(\partial_t + v_2\partial_x + \Gamma_2)a_2 = -\beta_2 a_0 a_1, \tag{13}$$

where x is the direction of propagation, and v_j, Γ_j, and $\beta_j > 0$ are the velocities, damping rates, and coupling parameters, respectively. Consider, in the following, solutions of Eq. (13) in the form of traveling waves $a_j = a_j(\xi)$, $\xi = x - ct$, with the velocity c undetermined. Upon substituting into Eq. (13), one arrives at

$$(\partial_\xi + \tilde{\Gamma}_0)a_0 = -\gamma_0 a_1 a_2, \tag{14a}$$

$$(\partial_\xi + \tilde{\Gamma}_1)a_1 = \gamma_1 a_0 a_2, \tag{14b}$$

$$(\partial_\xi + \tilde{\Gamma}_2)a_2 = -\gamma_2 a_0 a_1, \tag{14c}$$

where $\gamma_j = \beta_j/(v_j - c)$, $\tilde{\Gamma}_j = \Gamma_j/(v_j - c)$. From Eqs. (14a) and (14b) with the constraint $\tilde{\Gamma}_0 = \tilde{\Gamma}_1 \equiv \Gamma^*$, one obtains the equation $a_0^2/\gamma_0 + a_1^2/\gamma_1 = \alpha^2 \exp(-2\Gamma^*\xi)$, α being an arbitrary constant. This equation is satisfied by

$$a_0 = \alpha\sqrt{\gamma_0}e^{-\Gamma^*\xi}\cos(\Psi/2),$$

$$a_1 = \alpha\sqrt{\gamma_1}e^{-\Gamma^*\xi}\sin(\Psi/2), \tag{15}$$

where $\Psi = \Psi(\xi)$ remains to be determined. Upon substituting Eq. (15) into Eq. (14a), one gets

$$a_2 = (2\sqrt{\gamma_0\gamma_1})^{-1}\partial_\xi\Psi. \tag{16}$$

Finally, after substituting Eqs. (15) and (16) into Eq. (14c), one arrives at

$$\partial_{\xi\xi}\Psi + \tilde{\Gamma}_2\partial_\xi\Psi + \kappa^2 e^{-2\Gamma^*\xi}\sin\Psi = 0, \tag{17}$$

with $\kappa^2 \equiv \alpha^2\gamma_0\gamma_1\gamma_2$. Now, when the constraints $4\Gamma^* = \tilde{\Gamma}_2$, $v_j > c$ are satisfied, the aforementioned symmetry $\hat{S}_2$ implies that the solutions of Eq. (17) are those of the AR Eq. (6) under time reversal with the identifications $t \to \xi$, $\delta \to 3\tilde{\Gamma}_2/2$, $\omega_0 \to \kappa$. In particular, this yields

$$a_0(\xi) \approx \alpha\sqrt{\gamma_0}e^{-\Gamma^*\xi}\cos(\kappa^2 e^{-2\Gamma^*\xi} + \varphi),$$

$$a_1(\xi) \approx \alpha\sqrt{\gamma_1}e^{-\Gamma^*\xi}\sin(\kappa^2 e^{-2\Gamma^*\xi} + \varphi),$$

$$a_2(\xi) \approx -2\kappa^2\Gamma^*(\gamma_0\gamma_1)^{-1/2}e^{-2\Gamma^*\xi} \tag{18}$$

for $\xi > 1/\Gamma^*$ according to Eq. (7). Physically, this means that the amplitudes a_j are subjected to exponential decays for $\xi \gg 1/\Gamma^*$. In particular, one has the scalings $a_0(\xi \gg 1/\Gamma^*) \sim e^{-\Gamma^*\xi}$, $a_1(\xi \gg 1/\Gamma^*) \sim e^{-3\Gamma^*\xi}$, $a_2(\xi \gg 1/\Gamma^*) \sim e^{-2\Gamma^*\xi}$ for $\varphi = 0$. Note that the aforementioned constraints permit one to obtain the velocity $c = (v_0 - v_1\Gamma_0/\Gamma_1)(1 - \Gamma_0/\Gamma_1)^{-1}$ and are satisfied over regions of finite measure in the parameter space $\{\Gamma_j, v_j\}$, the case $v_0 = v_2$, $\Gamma_2 = 4\Gamma_0$, $1 > v_0/v_1 > \Gamma_0/\Gamma_1$ being an example.

B. Resistively and capacitively shunted junction

Consider now the application of the above AR analysis to the following resistively and capacitively shunted junction (RCSJ) model [13]

$$\frac{\hbar C}{2e}\frac{d^2\varphi}{dt^2} + \frac{\hbar}{2eR}\frac{d\varphi}{dt} + I_c\sin\varphi = I_{AR}(t), \tag{19}$$

where φ is the phase difference of the quantum mechanical wave functions of the superconductors defining the Josephson junction, R is the model shunting resistance, C is the magnitude of the junction capacitance, and I_c is the critical current, while $I_{AR}(t)$ represents the as yet undetermined AR current flowing through the junction. After rescaling time, Eq. (19) can be recast into the form

$$\frac{d^2\varphi}{dt'^2} + \frac{\hbar\tilde{\omega}_0}{2eR\sqrt{I_c}}\frac{d\varphi}{dt'} + I_c\sin\varphi = I_{AR}(t'), \tag{20}$$

where $t' \equiv \tilde{\omega}_0 t/\sqrt{I_c}$, $\tilde{\omega}_0 \equiv \sqrt{\frac{2eI_c}{\hbar C}}$ being the Josephson plasma frequency. Now, a comparison between Eqs. (20) and (3) with $f(t)=1$ indicates that the AR solutions of the RCSJ model before SC are governed by the equation

$$\frac{d^2\varphi}{dt'^2} + I_c \sin\varphi = \frac{\hbar\tilde{\omega}_0}{2eR\sqrt{I_c}}\frac{d\varphi}{dt'}. \qquad (21)$$

In particular, theorem 1 gives us (in terms of the original time variable) the following AR solutions of Eq. (21):

$$\varphi_{\mathrm{AR}}(t<\tau^*) \simeq A\exp\left(\frac{t}{2RC}\right)\sin(\Omega^* t+\varphi_0) \qquad (22)$$

and hence the AR currents are

$$I_{\mathrm{AR}}(t<\tau^*) \simeq \frac{A\hbar}{eR}\exp\left(\frac{t}{2RC}\right)\sin(\Omega^* t+\varphi_0+\Theta), \quad (23)$$

where $A(\ll 1)$, φ_0 are arbitrary constants, $\Omega^* \equiv \sqrt{\tilde{\omega}_0^2 - \frac{1}{2R^2C^2}}$, $\Theta \equiv \arctan(\sqrt{4R^2C^2\tilde{\omega}_0^2 - 2})$, while the escape time scales as $\tau^* \sim RC$, and $\tilde{\omega}_0 > \frac{1}{\sqrt{2}RC}$. Note that this relationship between the Josephson plasma frequency and the time constant RC (see theorem 2) represents a necessary condition for the phase difference of the quantum-mechanical wave functions to maximally increase along time according to Eq. (22) from an initial state very close to equilibrium when the current flowing through the junction is given by Eq. (23). The author is confident that Eqs. (22) and (23) can be successfully tested with an experiment involving a single Josephson junction. In this regard, a linear approximation for $\exp(\frac{t}{2RC})$ could be used since the escape time scales as $\tau^* \sim RC$.

C. Topological solitons in Frenkel-Kontorova chains

Consider now the problem of optimally accelerating a topological soliton, which is initially pinned to a certain pendulum, in a damped, driven Frenkel-Kontorova (FK) chain by AR external forces. This represents an ubiquitous problem since the FK model provides a fairly accurate description of diverse physical and biological phenomena and systems, including ladder networks of discrete Josephson junctions, charge density wave conductors, and DNA dynamics, to quote just a few [14]. For the sake of concreteness, the application of the EBAR theory is discussed in the following case:

$$\ddot{u}_j + \frac{K}{2\pi}\sin(2\pi u_j) = -\alpha\dot{u}_j + u_{j+1} - 2u_j + u_{j-1} - F_{\mathrm{AR}}(t''), \qquad (24)$$

where u_j is the phase of the jth pendulum, $\dot{u}_j \equiv du_j/dt''$, etc., K measures the strength of the substrate potential, α is the damping coefficient, and $F_{\mathrm{AR}}(t'')$ is the as yet undetermined AR force (where the minus sign is introduced for convenience). Also, a finite chain of N particles with the following boundary condition: $u_{j+N}=u_j+N+1$ is assumed to keep the analysis close to experimental realization (e.g., a circular array of Josephson junctions). As is well known, a collective coordinate formalism (CCF) [15] permits one to describe the motion of the soliton center of mass $X(t'')$ by means of an effective ODE, which is a perturbed pendulum for the FK model [16]. Thus, the application of CCF to Eq. (24) by assuming a sine-Gordon profile for the (discrete) soliton, $u_j = j \pm (2/\pi)\tan^{-1}\{\exp[j - X(t'')]/l_0\}$, yields the perturbed pendulum equation

$$\frac{d^2x}{dt^2} + \sin x = -\eta\frac{dx}{dt} + F_{\mathrm{AR}}(t), \qquad (25)$$

where $x \equiv 2\pi X$, $t \equiv \Omega_{\mathrm{PN}} t''$, $\eta \equiv \alpha\Omega_{\mathrm{PN}}^{-1}$, where Ω_{PN} and l_0 are the Peierls-Nabarro frequency and the soliton width, respectively $\{\Omega_{\mathrm{PN}}^2/(2\pi) = (\pi^3 + 2\pi^5 l_0^2)/[6l_0\sinh(\pi^2 l_0)]\}$. Now, a comparison between Eqs. (25) and (3) with $f(t)=1$ indicates that the AR solutions of the effective ODE describing the motion of the soliton center of mass before SC are governed by the equation

$$\frac{d^2x}{dt^2} + \sin x = \eta\frac{dx}{dt}. \qquad (26)$$

In particular, theorem 1 gives us (in terms of the original space-time variables) the following AR solutions of Eq. (26):

$$X_{\mathrm{AR}}(t''<\tau^{**}) \simeq \frac{A}{2\pi}\exp\left(\frac{\alpha t''}{2}\right)\sin(\Omega^{**}t''+\varphi_0), \quad (27)$$

and hence the AR forces are

$$F_{\mathrm{AR}}(t''<\tau^{**}) \simeq \frac{2\alpha A}{\Omega_{\mathrm{PN}}}\exp\left(\frac{\alpha t''}{2}\right)\sin(\Omega^{**}t''+\varphi_0+\Xi), \qquad (28)$$

where $A(\ll 1)$, φ_0 are arbitrary constants, $\Omega^{**} \equiv \sqrt{\Omega_{\mathrm{PN}}^2 - \frac{\alpha^2}{4}}$, $\Xi \equiv \arctan(\sqrt{4\Omega_{\mathrm{PN}}^2/\alpha^2 - 1})$, while the escape time scales as $\tau^{**} \sim \alpha^{-1}$ and $\Omega_{\mathrm{PN}} > \alpha/2$. This relationship between the Peierls-Nabarro frequency and the time constant α^{-1} (see theorem 2) represents a necessary condition for the topological soliton to optimally accelerate along time according to Eq. (27) from an initial pinned state very close to equilibrium when the external force acting on the FK chain is given by Eq. (28). Equations (27) and (28) can be successfully tested with an experiment involving a circular array of Josephson junctions, where a linear approximation for $\exp(\alpha t''/2)$ could be used since the escape time scales as $\tau^{**} \sim \alpha^{-1}$.

V. CONCLUSION

Optimal energy amplification via autoresonance in dissipative systems subjected to separatrix crossings has been discussed in the framework of the energy-based autoresonance theory through the universal model of a damped driven pendulum. Analytical expressions for autoresonance solutions and forces as well as for the associated adiabatic invariants inside and outside the underlying separatrix were deduced. Numerical studies supplement the autoresonance analysis and confirm the conclusions. Additionally, the autoresonance analysis has been applied to three relevant physical contexts: the three-wave problem in dissipative media, the resistively and capacitively shunted junction model, and the Frenkel-Kontorova model, where analytical predictions were deduced from the autoresonance analysis. These predictions can be tested experimentally, and the author hopes that this work will motivate several novel experiments. It should be stressed that the present results can be applied to virtually any physical scenario where a damped driven pendulum could appear as a suitable (effective or exact) dynamic model, the case of cold atoms in optical potentials, for instance, provides an additional example for future research.

ACKNOWLEDGMENTS

The author acknowledges financial support from the Spanish MCyT through the FIS2008-01383/FIS project.

[1] D. Bohm and L. Foldy, Phys. Rev. **70**, 249 (1946).
[2] R. Malhotra, Nature (London) **365**, 819 (1993).
[3] J. Fajans and L. Friedland, Am. J. Phys. **69**, 1096 (2001).
[4] W. K. Liu, B. Wu, and J. M. Yuan, Phys. Rev. Lett. **75**, 1292 (1995).
[5] R. Chacón, Europhys. Lett. **70**, 56 (2005).
[6] F. Cariello and M. Tabor, in *Painlevé Transcendents*, edited by D. Levi and P. Winternitz (Plenum, New York, 1992).
[7] A. J. Lichtenberg and M. A. Lieberman, *Regular and Chaotic Dynamics* (Springer, New York, 1992).
[8] The inclusion of $f(t)$ into Eq. (1) is motivated by the well-known phenomenon of parametric pumping. See, e.g., J. R. Sanmartín, Am. J. Phys. **52**, 937 (1984).
[9] P. F. Byrd and M. D. Friedman, *Handbook of Elliptic Integrals for Engineers and Scientists* (Springer-Verlag, Berlin, 1971).
[10] Notice that both AR equations, Eqs. (6) and (8), also present the equilibrium ($x_{\mathrm{AR}}=0$, $\dot{x}_{\mathrm{AR}}=0$) as a mathematical (formal) AR solution, in the sense that $x_{\mathrm{AR}}=0$ and the corresponding AR excitation $F_{\mathrm{AR}}\equiv 2\delta\dot{x}_{\mathrm{AR}}=0$ "trivially" have the same instantaneous period for all t. However, physically it is not an AR solution since the energy does not increase over time.
[11] H. Goldstein, *Classical Mechanics* (Addison-Wesley, Reading, 1980).
[12] K. Papadopoulos, K. Ko, and V. Tripathi, Phys. Rev. Lett. **51**, 463 (1983); R. H. Enns and S. S. Rangnekar, Phys. Status Solidi B **94**, 9 (1979).
[13] A. Barone and釘Paternó, *Physics and Applications of the Josephson Effect* (Wiley, New York, 1982).
[14] For extensive review of applications of the FK model, see L. Floría and J. J. Mazo, Adv. Phys. **45**, 505 (1996); and O. M. Braun and Y. S. Kivshar, Phys. Rep. **306**, 1 (1998), and references therein.
[15] C. Willis, M. El-Batanouny, and P. Stancioff, Phys. Rev. B **33**, 1904 (1986); M. K. Sayadi and J. Pouget, Physica D **55**, 259 (1992).
[16] P. J. Martínez and R. Chacón, Phys. Rev. Lett. **93**, 237006 (2004); Phys. Rev. Lett. **96**, 059903(E) (2006).